THE USE OF PERMEABILITY AND CAPILLARY THEORY TO CHARACTERIZE THE STRUCTURE OF WOOD AND MEMBRANE FILTERS[1]

J. F. Siau

Professor
Department of Wood Products Engineering, State University of New York
College of Environmental Science and Forestry, Syracuse, NY 13210

Y. Kanagawa

Faculty of Agriculture, Nagoya University
Chikusa, Nagoya, 464, Japan

and

J. A. Petty

Lecturer
University of Aberdeen, Department of Forestry, St. Machar Drive
Old Aberdeen AB9 2UU Scotland, U.K.

(Received 29 February 1980)

ABSTRACT

Air permeability and bubble point measurements were made with two sizes of Nuclepore filter membrane, six other membranes of relatively nonhomogeneous structure, and three wood specimens. Radii calculated from a plot of permeability vs. reciprocal pressure, from air flow and porosity, and from the bubble point were compared. The Nuclepore filters, typical of the uniform-parallel-circular capillary model, gave values of radii by the different methods which were in close agreement. The membranes had permeability vs. reciprocal pressure plots that were linear, indicating the absence of high and low conductances in series. The six relatively nonhomogeneous membranes gave radii that differed significantly when calculated by the different methods. The wood specimens had curvilinear plots of permeability vs. reciprocal pressure, indicating high and low conductivities in series and a more nonhomogeneous structure than any of the filters. The degree of disparity in the radii measured by the different methods can be taken as a measure of structural inhomogeneity.

Keywords: Permeability, gas flow, membrane filters, capillaries.

INTRODUCTION

Membrane filters have been used as models to investigate the use of the Adzumi or Klinkenberg equations (Siau 1971) for the calculation of the mean effective radii and the number of openings in the cross section of wood specimens (Petty 1974; Smith and Banks 1971). There are two principal types of membrane filters currently being produced. Nuclepore Corporation manufactures a membrane of polycarbonate in which bombardment in a nuclear reactor is used as a means of controlling the size and number of holes such that a close approximation to the ideal parallel-capillary model is obtained as revealed in Fig. 1 (a). Most of the other filters are extremely nonhomogeneous in structure, as evident from the

[1] This work was carried out at the University of Aberdeen while J. F. Siau was on sabbatical leave and was partially supported by the NATO Senior Scientists Programme, and at SUNY College of Environmental Science and Forestry, Syracuse while Y. Kanagawa was on sabbatical leave.

Gelman and Millipore filters depicted in Figs. 1 (b) and (c). They are intended primarily as filtration devices but, in a sense, their inhomogeneity has some utility in the study of wood with its very complex anatomical structure. It is useful, therefore, to examine and classify ways in which flow measurements may be used to elucidate and characterize structural inhomogeneities. One approach to the problem is to use flow theory, based upon the uniform-parallel-circular-capillary model to calculate the radius or pore size distribution by the different methods described below.

METHODS FOR DETERMINATION OF PORE SIZES

Viscous and slip flow measurements with a gas

The Adzumi equation (Siau 1971) may be rearranged in two ways to permit calculation of the mean effective pore radius (r) by dividing the viscous term (proportional to r^4) by the slip-flow term (proportional to r^3). In the first method employed by Petty (1974), the equation is rearranged with the flow rate (Q) at pressure (P) per unit pressure differential (Q P/ΔP) as the dependent variable and the average pressure ($\bar{P}$) as the independent variable. The radius can then be calculated by dividing the slope of the linear plot of Q P/ΔP vs. $\bar{P}$ by the intercept. In the second method, the Adzumi equation may be rearranged with conductance (Q P/ΔP $\bar{P}$) or permeability (K_g) as the dependent variable and reciprocal average pressure ($1/\bar{P}$) as the independent variable. When permeability is the dependent variable, it is called the Klinkenberg equation.

$$K_g = K(1 + (0.4 \times 10^{-4} \text{ atm cm})(r\bar{P})^{-1}) = Ks \quad (1)$$

where K_g = specific gas permeability
K = intercept specific gas permeability at infinite pressure
$\bar{P}$ = average pressure, atm
r = radius, cm
s = slip flow factor

The constant, 0.4×10^{-4} atm cm is based upon air flow under standard conditions. If SI units were used, the constant would be written as 4.0×10^{-10} Pa m.

The slip-flow factor represents the factor by which the viscous-flow term is increased at a given average pressure due to the slip-flow component. It is evident from Eq. (1) that "s" approaches a limiting minimum value of unity as the average pressure increases. Also it is significantly greater than unity when the mean free path of the gas molecules is in the order of the radius of the capillary.

When a linear plot of K_g vs. $1/\bar{P}$ is made in accordance with Eq. (1), it is clear that the mean effective radius may be calculated from the following relationship.

$$r = 0.4 \times 10^{-4} \text{ atm cm} \times (\text{intercept/slope}) \quad (2)$$

Petty (1970) has found a curvilinear relationship between permeability and reciprocal pressure for woods, rather than the linear relationship predicted by the Klinkenberg equation. He has attributed this phenomenon to the effect of two or more conductances in series. If two conductances are assumed, each of which obeys the Klinkenberg equation, the relationship between permeability and reciprocal pressure has the form:

$$K_g = [(M/\bar{P} + B)(L/\bar{P} + A)]/(M/\bar{P} + L/\bar{P} + B + A) \quad (3)$$

where M and L are the slopes of two linear Klinkenberg plots representative of radii of different sizes. B and A are intercepts of these plots, respectively.

If it is assumed that L is the smaller slope corresponding with the largest radius, e.g. that of the tracheid cell lumen, then the large radius (r_1) may be calculated as:

$$r_1 = 0.4 \times 10^{-4} \text{ atm cm} \times (A/L) \tag{4}$$

If M and B represent the slope and intercept for the small radius, the Clausing factor becomes important because the ratio of membrane thickness (L_p) to radius is small for pit openings. Petty (1970) shows that the calculation of the small radius requires the use of a quadratic equation when the Clausing factor is included. In the case where the ratio, L_p/r_2, is near unity, the Clausing factor (K_c) is equal to $(1 + L_p/2r)^{-1}$ to a close approximation. The equation for calculation of r_2 may be then written as:

$$r_2/L_p = -0.25 + \sqrt{0.0625 + 1.9 \times 10^{-5} \text{ atm cm} \times (B/ML_p)} \tag{5}$$

where L_p = thickness of membrane.

Petty (1970) has applied Eq. (5) to calculate the radius of the pit openings in softwoods and Eq. (4) to determine the tracheid diameters. The values of A, B, L, and M can be calculated from the data of K_g vs. $1/\bar{P}$ by means of a curve-fitting program with a digital computer.

Bubble point test

This is specified by ASTM (1970) as a standard test for the measurement of the maximum pore size of a membrane filter. One surface of the membrane is submerged in a liquid and a gradually increasing air pressure is applied to the other surface until a steady stream of bubbles is observed in the liquid. This final pressure is used to calculate the radius by use of the following fundamental relationship:

$$r = 2\gamma \cos \theta/\Delta P \tag{6}$$

where γ = surface tension
θ = contact angle
ΔP = pressure differential required to displace the air-liquid meniscus

Stamm (1964) used this method to determine the maximum radius of pit openings and tracheid lumens in softwoods. Stamm (1966) and Jacobs (1972) have also applied it to membrane filters.

If it is assumed that $\theta = 0°$ for an air-water meniscus across an opening in the membrane, Eq. (6) may be simplified to the form:

$$r = (21.4(\mu\text{m lb})/\text{in}^2)/\Delta P \tag{7}$$

→

FIG. 1. (a) Nuclepore N 020 membrane filter. Arrows indicate multiple openings which account for low bubble point pressure. (b) Gelman GA-8 membrane filter, (c) Millipore GS membrane filter, (d) Cross section of *Tilia americana* L. (basswood), (e) Cross section of *Acer saccharum* Marsh (sugar maple), (f) Cross section of *Pinus lambertana* Dougl. (sugar pine).

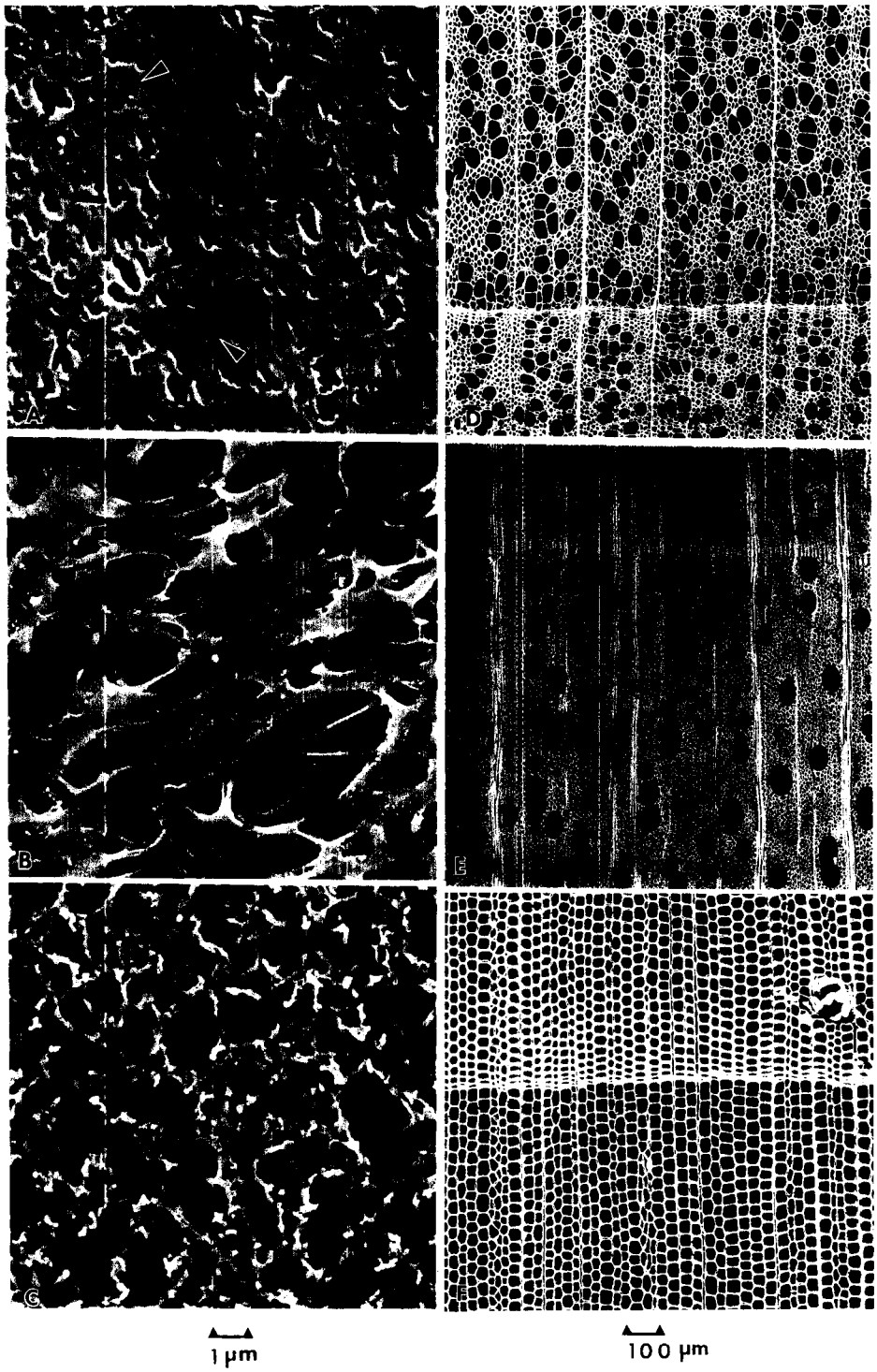
A
B
C
D
E
1 µm
100 µm

where r = radius of opening, μm
ΔP = pressure differential, lb/in^2

ASTM (1970) assigns a value of 15.0 rather than 21.4 as given in Eq. (7), thus introducing a "capillary constant" of 0.7. Bechold (1908) assigns limits of 0.1 to 1.0 to such a constant. The reason for the selection of 0.7 is not discussed in the ASTM specification. Accordingly, radii are calculated in this investigation using the following equation:

$$r = 15(\mu m\ lb)/in^2/\Delta P \quad (8)$$

Equation (8) could be converted to SI units by substitution of 1.03×10^5 μm Pa for the constant.

Mercury porosimetry

Mercury is forced into a porous substance under a measured pressure differential that is a function of the radius, surface tension, and contact angle according to Eq. (6). Assuming a surface tension of 435 dyne/cm and a contact angle with wood of 130°, a simplified equation of the form of Eq. (7) may be derived where r is expressed in micrometers and ΔP in lb/in^2.

$$r = 90(\mu m\ lb)/in^2/\Delta P \quad (9)$$

When this method is employed, data of volume of mercury forced into wood vs. pressure are recorded. The pressure is related to a radius through Eq. (9) and the pore-size distribution may be calculated from the volumetric flow data. This has been done with wood by Stayton and Hart (1965) and Blankenhorn et al. (1978).

Gas flow through a wetted membrane

This method is similar to the bubble point test except that additional provisions are made to measure the rate of gas flow through the membrane as the air pressure is gradually increased to force it through successively smaller openings [ASTM (1970)]. A curved plot of Q (flow rate) vs. ΔP is obtained through the wet membrane in contrast with the linear plot for flow through a dry filter in accordance with the Adzumi equation. A flow-average radius is calculated by dividing the slope of the dry-air plot of Q vs. ΔP by 2.0 and superimposing this result on the wet-flow plot of Q vs. ΔP. The intersection occurs at a value of ΔP which corresponds with the flow-average radius as calculated by Eq. (8). This radius has the physical significance that half of the flow through the dry membrane occurs through radii of smaller size and half through radii of larger size than the flow-average radius.

Extending this procedure, it is possible to calculate the distribution of pore sizes in a membrane by finding intersections of the wet-flow curve with straight lines representing various ranges of fractional flow rates. The result is a flow-related pore-size distribution.

Fluid flow method

When the Hagen-Poiseuille equation is combined with the Darcy law equation, permeability is a function of the number and radius of the openings.

TABLE 1. *Comparison of flow properties of membrane filters—r in micrometers.*

Filter type	r specified	V_a spec.	K darcy	r Klinkenberg plot eq. (1)	r air flow eq. (11)	r K. plot / r air flow	r from spec. bubble point eq. (8)	r K. plot / r B.P.
Sartorius 11311	*0.005	0.65	2.5×10^{-4}	0.12	0.055	2.2		
Sartorius 11311	*0.05							
Millipore VM	0.025	0.72	4.5×10^{-4}	0.14	0.070	2.0	0.040	3.5
Millipore GS	0.11	0.75	7.0×10^{-3}	0.35	0.27	1.3	0.28	1.2
Millipore WS	1.5		2.5×10^{-2}	0.65	0.51	1.3	1.3	0.5
Gelman GA-8	0.1	0.85	7.3×10^{-3}	0.43	0.26	1.7	0.30	1.4
Gelman GA-6	0.225	0.85	2.4×10^{-2}	0.82	0.47	1.7	0.68	1.2
Nuclepore N 020	0.09	0.076	3.2×10^{-4}	0.14	0.18	0.78	0.25	0.6
Nuclepore N 800	3.6	0.041	4.4×10^{-2}	3.2	2.9	1.1	7.5	0.4

* By mercury porosimetry and air flow respectively.

$$K = (n\pi r^4)/8 \tag{10}$$

where K = specific permeability, cm^2
n = no. of openings per cm^2 of cross section

In the parallel-capillary model the porosity, V_a, becomes equal to $n\pi r^2$, the fractional cross-sectional area of the capillaries. Making this substitution and solving for r:

$$r = \sqrt{(K \times 7.9 \times 10^{-8}\ cm^2/darcy)/V_a} \tag{11}$$

where r = radius, cm
K = intercept permeability, darcy

EXPERIMENTAL PROCEDURE

The air permeabilities of eight membrane filters (Tables 1 and 2) and three wood specimens (Table 3) were measured at reciprocal pressures from 1.2 to 24 atm^{-1} using the procedure described by Petty (1970). Two of the membrane filters were Nuclepore filters selected because their structure closely approximates the uniform-parallel-circular-capillary model. The other membrane filters were of a relatively nonhomogeneous structure. Also one specimen each of two hardwoods, *Tilia americana* L. (basswood) and *Acer saccharum* Marsh. (sugar maple) and one softwood, *Pinus lambertana* Dougl. (sugar pine) were selected to permit the investigation of various kinds of wood structure. The wood specimens were 2.5 cm in diameter and 4.5 cm long and permeability was measured in the longitudinal

TABLE 2. *Characteristics of Nuclepore filters—values of n in* cm^{-2}.

Specified r micrometers	Specified n	n figure 1(a)	n from K and specified r eq. (10)
0.09	3×10^8	2.9×10^8	2.1×10^8
3.6	1×10^5		0.66×10^5

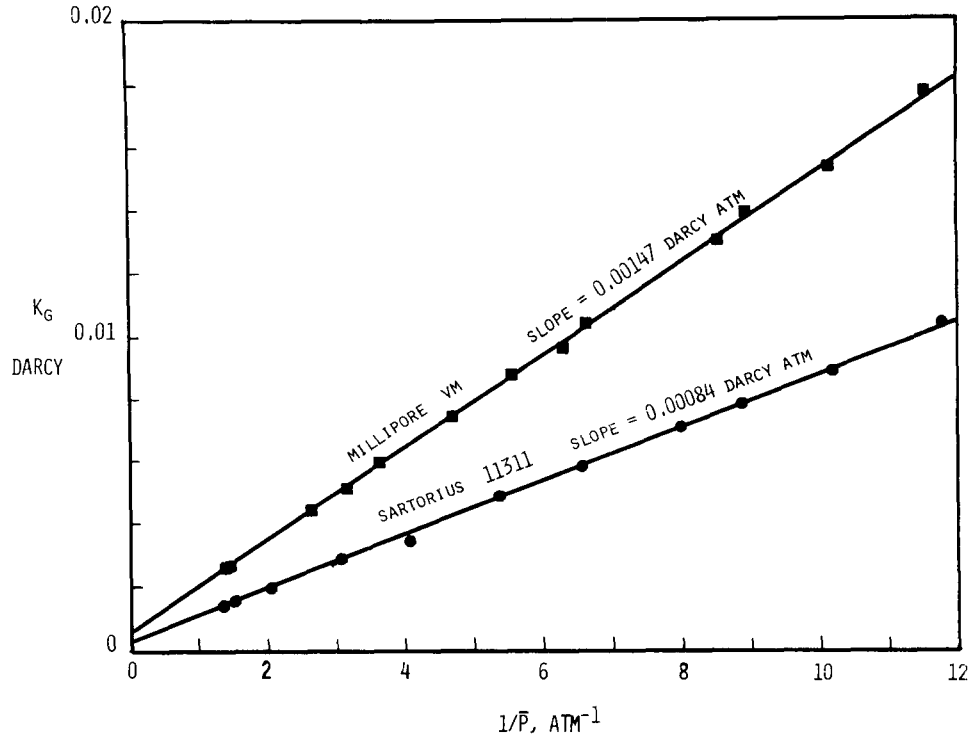

FIG. 2. Permeability vs. reciprocal pressure for Millipore VM and Sartorius 11311 membrane filters.

direction. Typical Klinkenberg plots of K_g vs. $1/\bar{P}$ of the membrane filters are revealed in Fig. 2, and of the wood specimens in Fig. 3. The plot for sugar pine was not included in the latter because the two plots provided are typical of the results obtained with wood specimens.

Linear plots of K_g vs. $1/\bar{P}$ were obtained for all the membrane filters. The mean-effective radii were calculated using Eq. (2) with the application of the Clausing factor and Couette correction where required [Petty (1974)] in the case of thin, orifice-like openings. Measurements with the wood specimens resulted in curvilinear plots as indicated in Fig. 3. The equations of these plots were determined in the form of Eq. (3) using curve-fitting techniques. The values of the large and small radii were then calculated from Eq. (4) and (5). The thickness of the pit membranes (L_p) was assumed to be 0.1 micrometer in agreement with the value selected by Petty (1970). The radii of all the specimens were calculated by the fluid-flow method from the porosity and intercept permeability using Eq. (11). The bubble test was applied to the wood to determine the size of the vessels in the hardwoods and the tracheids and pit openings of the sugar pine specimen. The ends of the cylindrical specimens were placed in water, and the air pressure was gradually increased until bubbles first appeared to determine vessel and tracheid sizes. The radius was calculated from Eq. (8). An additional test was made with the sugar pine after impregnation with water using the full-cell vacuum process for the purpose of filling the tracheids and resin canals. The pressure

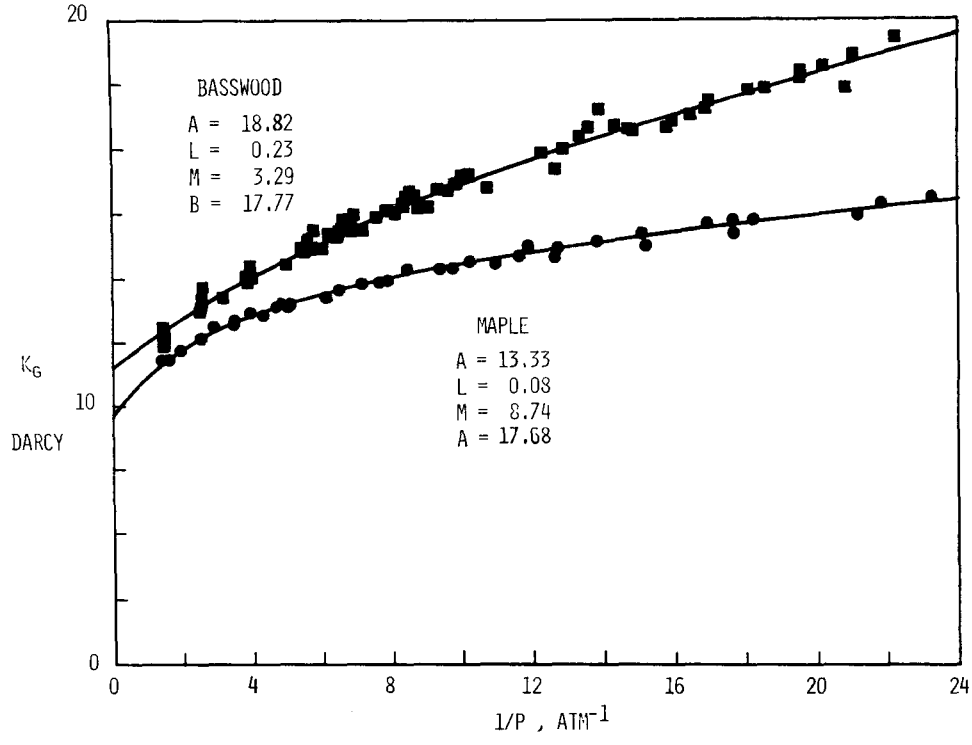

FIG. 3. Permeability vs. reciprocal pressure for basswood and sugar maple wood specimens.

then had to be increased to a much greater value which was assumed to be that required to force bubbles through the pit openings. The radii of vessels and tracheids were also measured from the scanning electron micrographs for comparison with the values calculated by the other methods. The porosities of the wood specimens were calculated from the densities [Siau (1971)]. In addition to this the number of openings per unit area (n) and the average radius (r) of the Nuclepore N 020 membrane filter were measured from Fig. 1 (a) for comparison with the values calculated by other methods.

The permeability measurements of the membrane filters were done at University of Aberdeen and the work with the wood specimens and the scanning electron micrographs were completed at SUNY College of Environmental Science and Forestry.

RESULTS AND DISCUSSION

The plots of K_g vs. $1/\bar{P}$ for all the membrane filters were linear and typical of those revealed in Fig. 2. This linearity indicates that the flow is in accordance with the Klinkenberg equation and therefore it can be concluded that there is no nonlinear flow which could result from turbulent flow or kinetic energy losses where the air enters the membrane (Siau and Petty 1979). These linear plots also indicate that there was no significant presence of high and low conductances

TABLE 3. *Flow properties of wood specimens—r in micrometers.*

Wood species	r vessel or tracheid, SEM	V_a calc. from density	K darcy	r plot of K_g vs. $1/\bar{P}$ eq. (4) & (5)	r air flow eq. (11)	Ratio r plot / r air flow	r bubble point eq. (8)	Ratio r plot / r B.P.
Basswood	14–41 (Vessels)	0.72	9.1	$r_1 = 32.9$ $r_2 = 0.17$	10.0	3.23 0.017	32.1	1.02
Sugar maple	18–68 (Vessels)	0.58	7.6	$r_1 = 64.7$ $r_2 = 0.34$	10.2	6.34 0.034	23.3	2.78
Sugar pine	12–28 (Tracheids) 64 (Resin canal)	0.78	0.23	$r_1 = 20.2$ $r_2 = 0.30$	1.5	13.5 0.20	30.9 1.3	0.65 0.23

in series as found in wood by Petty (1970), and as indicated by the curved plots in Fig. 3.

Reference to Table 1 indicates that there was relatively good agreement between radii calculated from the Klinkenberg plot and by the air-flow method for the Nuclepore filters. The radii calculated from the bubble point for the Nuclepore filters were approximately two to three times those by the other methods. Figure 1 (a) reveals that the Nuclepore filters closely approximate the parallel-capillary model, with the circular holes of nearly the same size. The occasional overlapping of bombardments resulted in some much larger holes as indicated by the arrows, explaining the high values obtained by calculation from the specified bubble points. In addition to these calculations for the Nuclepore filters, the manufacturer has specified the value of "n" and this can be compared with a value calculated from the permeability using Eq. (10) and with a value determined from the scanning electronmicrograph (Fig. 1a). Table 2 reveals a relatively good agreement between the various values of "n." It is concluded that the Nuclepore filters closely approximate the uniform-parallel-circular-capillary model.

In regard to the nonhomogeneous membrane filters manufactured by Sartorius, Millipore, and Gelman, it is clear from Table 1 that there are larger differences between the various radii than in the case of the Nuclepore filters. Figures 1 (b) and (c) also illustrate their nonhomogeneity. The linear Klinkenberg plots obtained in all cases are evidence that the widely differing opening sizes in the membranes behave as though they are in parallel rather than in series when their effect on the flow is considered. Large and small openings in series result in a curvilinear plot of K_g vs. $1/\bar{P}$, as in Fig. 3, provided there is a sufficient difference in the conductivities such as that found between tracheid lumens and pit openings in softwoods or between vessels and intervessel pits in hardwoods. The ratio of radii determined from the Klinkenberg plot to that from air flow tends to increase as the specified radius decreases suggesting an increased nonhomogeneity with decreased opening size. It is difficult to compare specified radii with the other values for these filters because they are determined by different methods by the various manufacturers. This is evident from the two specified values for the Sartorius filter where 0.005 μm was determined by mercury porosimetry and 0.05 μm by air flow. This wide difference could be attributed to the nonhomogeneous structure. The mercury porosimetry value would be influenced by the smallest

portion of an opening encountered as mercury is forced through the filter, while the air flow value would be influenced by the widest portion of the opening because air flow increases as the fourth power of the radius. Large differences are also evident between radii calculated from the Klinkenberg plots and the specified bubble points. It can be concluded that the wide differences in radii determined by different methods for these filters are evidence of a wide departure from the uniform-circular-parallel-capillary model, particularly in membrane filters with the smallest openings. Thus greater differences in radii calculated by different methods are a measure of increased nonhomogeneity.

The results obtained for the wood specimens are revealed in Table 3 where the ranges of values measured from the scanning electronmicrographs are given for comparison with the other values obtained by the other methods. The radii calculated from the bubble point and the large radii (r_1) from the Klinkenberg plot are within these ranges for all the woods if large radius of the resin canal in sugar pine is considered. Therefore, a reasonable agreement is obtained between the large radii determined by the three methods when the high degree of nonhomogeneity of wood structure is considered.

The value of the small radius (r_2) obtained for sugar pine of 0.30 μm is a reasonable value for the pit openings between the tracheids. The higher value of 1.3 μm calculated from the bubble point is probably typical of the largest of these pit openings. In the case of the hardwoods, the values of r_2 could not be due to the resistance of perforation plates between the vessel elements because both basswood and sugar maple have simple perforation plates with large openings which would not be expected to produce a curvilinear plot. The small values of 0.17 and 0.34 μm could be interpreted as intervessel pits because of the limited length of vessels in diffuse-porous hardwoods.

The radii calculated from the air flow using the porosity and permeability with Eq. (11) are intermediate between the values of r_1 and r_2 calculated from the plots. In the case of the hardwoods, this could be explained by the fact that most of the flow occurred through the vessels whose volume fraction was much lower than the porosity of the wood. In the case of the sugar pine, the very low air flow value can be attributed to the high resistance of the pit openings, which are in series with the tracheids. The ratios of the radii calculated from the plots and those by air flow are very high when r_2 is used and low when r_1 is used. In nearly all cases, the disparity between the values is much greater for wood than for the membrane filters indicating a higher degree of nonhomogeneity in the wood specimens.

In conclusion it can be stated that the differences in values of radius in a porous solid determined by various methods can be used as a measure of their deviations from the ideal parallel-circular-capillary model. The Nuclepore filters are the closest to the ideal, followed by the nonhomogeneous filters produced by Millipore, Sartorius, and Gelman. In the latter cases, linear plots of K_g vs. $1/\bar{P}$ indicated that the various sized openings behave as if they are in parallel rather than in series as in wood. Finally, the wood specimens are the most nonhomogeneous because of their curvilinear plots and the wide disparity between radii determined by the various methods.

REFERENCES

ASTM. 1970. Standard test method for pore size characteristics of membrane filters for use with aerospace fluids. ASTM F 316-70. Annual Book of ASTM Standards Part 41:684–690.

BECHOLD, H. 1908. Durchlassigkeit von Ultrafiltern. Zeitschr. Physik Chemie 64:328–343.

BLANKENHORN, P. R., D. P. BARNES, D. E. KLINE, AND W. K. MURPHEY. 1978. Porosity and pore size distribution of black cherry carbonized in an inert atmosphere. Wood Sci. 11(1):23–29.

JACOBS, S. 1972. The distribution of pore diameters in graded ultrafilter membranes. Filtration and Separation. September/October:525–530.

PETTY, J. A. 1970. Permeability and structure of the wood of Sitka spruce. Proc. Roy. Soc. Lond. B 175:149–166.

———. 1974. Laminar flow through short capillaries in conifer wood. Wood Sci. Technol. 8:275–282.

SIAU, J. F. 1971. Flow in wood. Syracuse University Press: Ch. 1 and 3.

SMITH D. N. R., AND W. B. BANKS. 1971. The mechanism of flow of gases through coniferous wood. Proc. Roy. Soc. Lond. B 177:197–223.

STAMM, A. J. 1964. Wood and cellulose science. Ronald: Ch. 22.

———. 1966. Maximum pore diameters of film materials. For. Prod. J. 16(12):59–63.

STAYTON, C. L., AND C. A. HART. 1965. Determining pore-size distribution in softwoods with a mercury porosimeter. For. Prod. J. 15(10):435–440.